Supplementary Information (SI) for Journal of Materials Chemistry A.

Heptazine-based conjugated microporous polymers for enhanced light absorption and charge separation in photocatalytic hydrogen peroxide production

Meng-Ran Zhang,[ab] *Su-Xian Yuan,*[ab] *You-Xiang Feng,*[a] *Min Zhang**[a] *and Tong-Bu Lu*[a]

[a]Institute for New Energy Materials and Low-Carbon Technologies, Tianjin University of Technology, Tianjin, 300384, China. Email: zm2016@email.tjut.edu.cn (M. Zhang)
[b]These authors contributed equally to this work.

Table of Contents

1. Materials and instrumentation

1.1 Materials

4,4′-Diamino-p-terphenyl (DPTP), 2,4,6-tris(4-formylphenyl)-1,3,5-triazine (TFPT) and acetic anhydride were supplied by Leyan Technology Co., Ltd. Melamine (99%), anhydrous aluminum chloride (≥98%), chromium trioxide (99%), xylene (≥99%), 1,3,5-trimethylbenzene (97%) and 1,2-dichlorobenzene (98%) were purchased from Shanghai Aladdin Biochemical Technology Co., Ltd. Potassium hydroxide (90%), phosphorus pentachloride (98%), acetic acid (99.5%), *N*,*N*-dimethylformamide (DMF, 99%) and tetrahydrofuran (THF, 99%) were gained from Shanghai Macklin Biochemical Co., Ltd. Ethanol (99.5%), sulfuric acid (98.3%) and dichloromethane (≥99.5%) were provided by Adamas-beta. Toluene (≥99.5%) was bought from Sinopharm Group Co., Ltd. Ethyl acetate (≥95%) was supplied by Innochem (Beijing) Technology Co., Ltd. 1,4-Dioxane (90.5%) was purchased from Fuchen (Tianjin) Chemical Reagent Co., Ltd. Deuterated solvents for nuclear magnetic resonance (NMR) spectroscopy measurements were sourced from Adamas-beta. Ultrapure water with a resistivity of 18.2 MΩ·cm was produced using a Milli-Q water purification system. All chemicals were used as received without further purification.

1.2 Instrumentation

Powder X-ray diffraction (XRD) patterns were recorded on a Rigaku SmartLab diffractometer (9 kW, Rigaku, Japan) with Cu Kα radiation (λ = 0.15418 nm) over a scan range from 3° to 30°. Fourier transform infrared (FTIR) spectra were acquired on a PerkinElmer Frontier spectrometer under ambient conditions. High-resolution transmission electron microscopy (HRTEM) images were captured using a FEI Talos F200X microscope. Thermogravimetric (TG) measurements were performed on a Netzsch TG-209 analyzer under an argon atmosphere. UV−visible diffuse reflectance spectra (UV−Vis DRS) were measured on a PerkinElmer Lambda 750 UV/VIS/NIR spectrophotometer. Nitrogen adsorption−desorption measurements were performed on Micromeritics ASAP 2020 and Microtrac BEL BELSORP-Mas analyzers. X-ray photoelectron spectroscopy (XPS) measurements were performed on a Thermo Scientific ESCALAB 250 Xi X-ray photoelectron spectrometer with Al Kα excitation. Water contact angles were determined on an SZ-CAMC33 contact angle goniometer. Photoelectrochemical measurements, including transient photocurrent response, electrochemical impedance spectroscopy, and Mott−Schottky analysis, were carried out on a CHI 760E electrochemical workstation. Photocatalytic experiments were performed under simulated solar illumination provided by a 300 W Xenon Lamp equipped with a 400 nm cut-off filter (CEL-HXF300).

The concentration of H_2O_2 in the reaction solution was determined via the colorimetric method using a U-3900 spectrophotometer. Reaction intermediates were monitored by in situ diffuse reflectance infrared Fourier transform spectroscopy (in situ DRIFTS) on a Thermo Scientific Nicolet iS50 instrument. Electron paramagnetic resonance (EPR) signals were recorded on a Bruker EMXplus-6/1 spectrometer. Photoluminescence (PL) spectra were collected using a Hitachi F-4600 fluorescence spectrophotometer.

2. Synthesis

2.1 Synthesis and characterization of monomer

1,3,3a[1],4,6,7,9-heptaazaphenalene-2,5,8-triyltris(benzene-4,1-diyl)tris(methanetriyl)hexaacetate (HEP-OAc) was prepared following the previously reported procedure, and its structure was confirmed via the ^{1}H nuclear magnetic resonance (^{1}H NMR) and ^{13}C NMR spectra. The synthetic route of HEP-OAc is illustrated in Scheme S1, with detailed procedures provided in the subsequent sections.

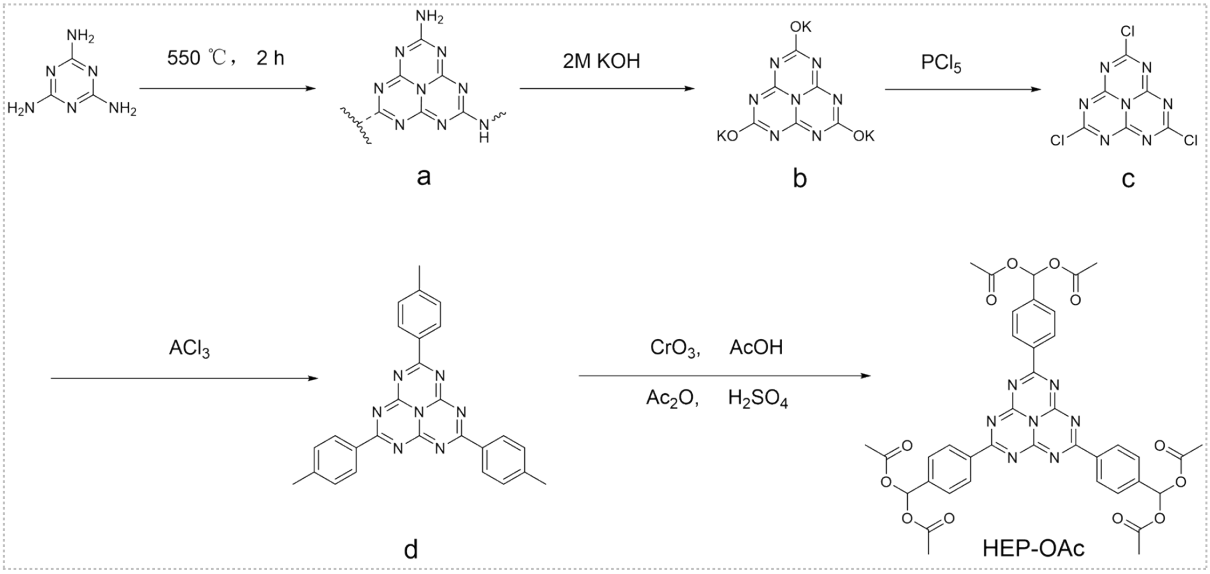

Scheme S1. Synthetic route of HEP-OAc.

2.1.1 Synthesis of hydrogenated g-C_3N_4 (a)

According to the previous reports,[1,2] intermediate **a** was synthesized via thermal treatment of 1,3,5-triazine-2,4,6-triamine (56.8 g, 0.45 mol) in a quartz tube furnace at 550 °C for 2 h. After cooling to ambient temperature, the faint yellow crude material was isolated and successively washed with ethanol and ethyl acetate, yielding 29.42 g (60%) of the target compound as a yellow powder.

2.1.2 Synthesis of 2,5,8-tris(potassium)cyamelurate (b)[2]

A clear solution was obtained by heating a mixture of hydrogenated g-C_3N_4 (10.0 g, 45.83 mmol) and 2 M KOH aqueous solution (300 mL) at 110 °C in a 500 mL two-necked flask. The resulting solution was filtered immediately while hot, and after the filtrate cooled to room temperature, 400 mL of anhydrous ethanol was added to induce product precipitation. The resulting white solid was isolated by filtration and dried at 80 °C overnight, yielding 11.24 g (71%) of pure material.

2.1.3 Synthesis of cyameluric chloride (c)[1–3]

Cyameluric chloride was synthesized by heating a mixture of 2,5,8-tris(potassium)cyamelurate (9.6 g, 28.62 mmol) and PCl_5 (17.6 g, 84.52 mmol) at 130 °C for 12 h with stirring in a 250 mL two-necked flask under nitrogen protection. After cooling to ambient temperature, the crude product was subjected to purification via Soxhlet extraction with anhydrous toluene for 48 h, followed by rotary evaporation to afford the final compound as a solid (5.9 g, 75% yield).

^{13}C NMR (DMSO-d_6, 100 MHz): δ (ppm) 151.85, 149.68.

2.1.4 Synthesis of tris-(4-tolyl)-tri-s-triazine (d)[1,4]

A 100 mL two-necked flask was charged with aluminum chloride (8.8 g, 65.92 mmol) and toluene (24 mL), and the mixture was heated to 60 °C under stirring. Cyameluric chloride (4.0 g, 14.47 mmol) was then added in portions, and the reaction was maintained at this temperature for 5 h, during which the color changed from yellow to red. After cooling to ambient temperature, the mixture was quenched by slowly adding ice water under stirring for 5 min. The resulting solid was collected by filtration and recrystallized from xylene to afford the product as a yellow powder (4.9 g, 76% yield).

^{1}H NMR ($CDCl_3$, 400 MHz): δ (ppm) 2.46 (s, 9H), 7.32 (d, J = 8.0 Hz, 6H), 8.47 (d, J = 8.0 Hz, 6H).

2.1.5 Synthesis of HEP-OAc[1]

HEP-OAc was synthesized through oxidation of tris-(4-tolyl)-tri-s-triazine (638 mg, 1.44 mmol) in a 100 mL two-necked flask. The reaction was carried out in a mixture of acetic anhydride (16 mL), acetic acid (24 mL), and H_2SO_4 (1.6 mL) maintained at 0 °C. Chromium trioxide (1.2 g, 12 mmol), finely ground into powder, was introduced gradually into the reaction system, and the resulting mixture was stirred for 30 min at 0 °C. After quenching with water, the mixture was filtered, and the crude product was purified by column chromatography using ethyl acetate/dichloromethane (1:1, *v*/*v*) as

eluent. The target compound was isolated as a yellow solid (253 mg, 22%) after rotary evaporation. ^{1}H NMR ($CDCl_3$, 400 MHz): δ (ppm) 2.18 (s, 18H), 7.67 (d, J = 8.0 Hz, 6H), 7.76 (s, 3H), 8.62 (d, J = 8.0 Hz, 6H).

^{13}C NMR ($CDCl_3$, 100 MHz): δ (ppm) 21.03, 88.97, 127.10, 130.96, 135.09, 141.75, 158.97, 168.90, 175.53.

2.2 Synthesis of Tt-CMP

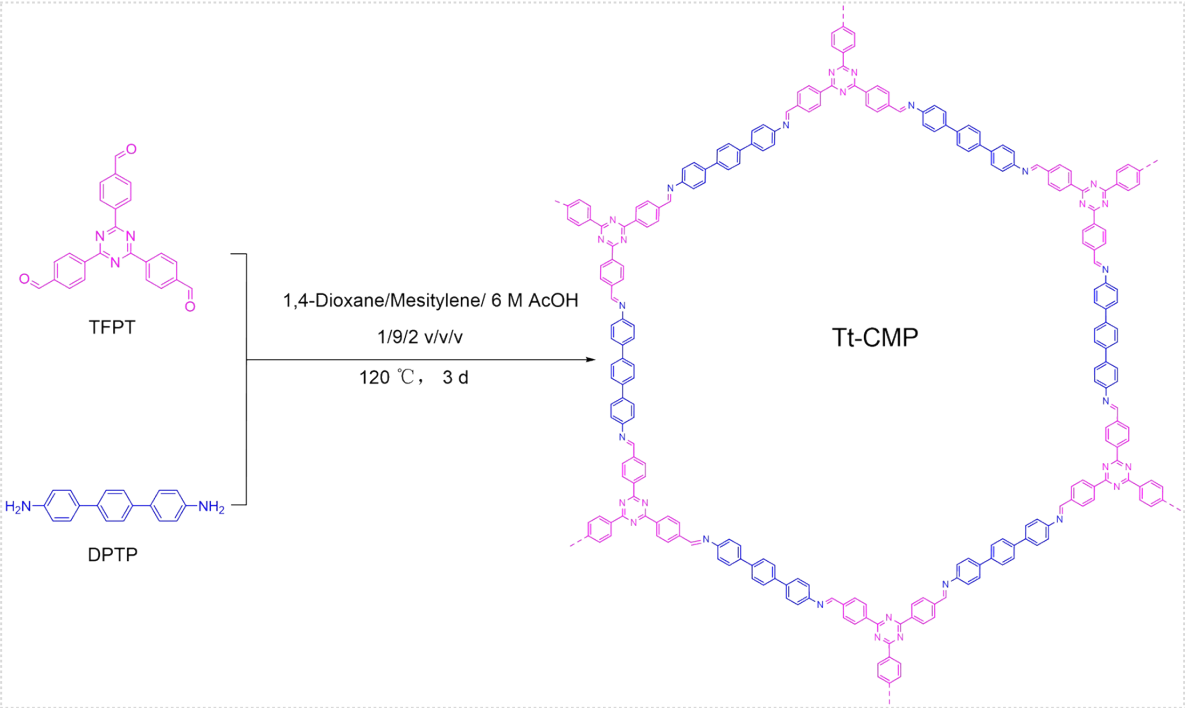

Scheme S2. Synthetic route of Tt-CMP.

TFPT-CHO (0.02 mmol, 7.90 mg) and DPTP (0.03 mmol, 7.80 mg) were placed in a 2 mL Pyrex tube, to which a mixed solvent system of 1,4-dioxane (0.1 mL) and mesitylene (0.9 mL) was added. After ultrasonication for complete mixing, 6 M acetic acid (0.2 mL) was introduced as a catalyst. The mixture was further sonicated for 10 min to ensure homogeneous dispersion of the monomers. The reaction system was then subjected to three freeze−pump−thaw cycles under liquid nitrogen and subsequently flame-sealed under vacuum. After the sealed tube was warmed to room temperature, it was transferred to an oven and maintained at 120 °C for 72 h. Upon completion of the reaction, the solid product was collected by vacuum filtration and successively washed with DMF and THF. The resulting solid was dried under vacuum at 80 °C for 24 h, affording a yellow fluffy powder in 88.2% yield.

2.3 Synthesis of Th-CMP

In a 2 mL Pyrex reaction tube, HEP-OAc (0.02 mmol, 15.84 mg) and DPTP (0.03 mmol, 7.80 mg) were combined with a mixed solvent system consisting of 1,4-dioxane (0.8 mL) and mesitylene (0.2 mL). After sonication to achieve complete mixing, 6 M acetic acid (0.2 mL) was introduced as a catalyst. The mixture was further sonicated for 10 min to ensure homogeneous dispersion of the monomers. The reaction system was then subjected to three freeze−pump−thaw cycles using liquid nitrogen, followed by flame-sealing of the Pyrex tube under vacuum. After warming to room temperature, the sealed tube was placed in an oven and maintained at 120 °C for 72 h. Upon completion of the reaction, the solid product was collected by vacuum filtration and thoroughly washed with DMF and THF. The resulting solid was dried under vacuum at 80 °C for 24 h, affording a tan-colored powder in 58.6% yield.

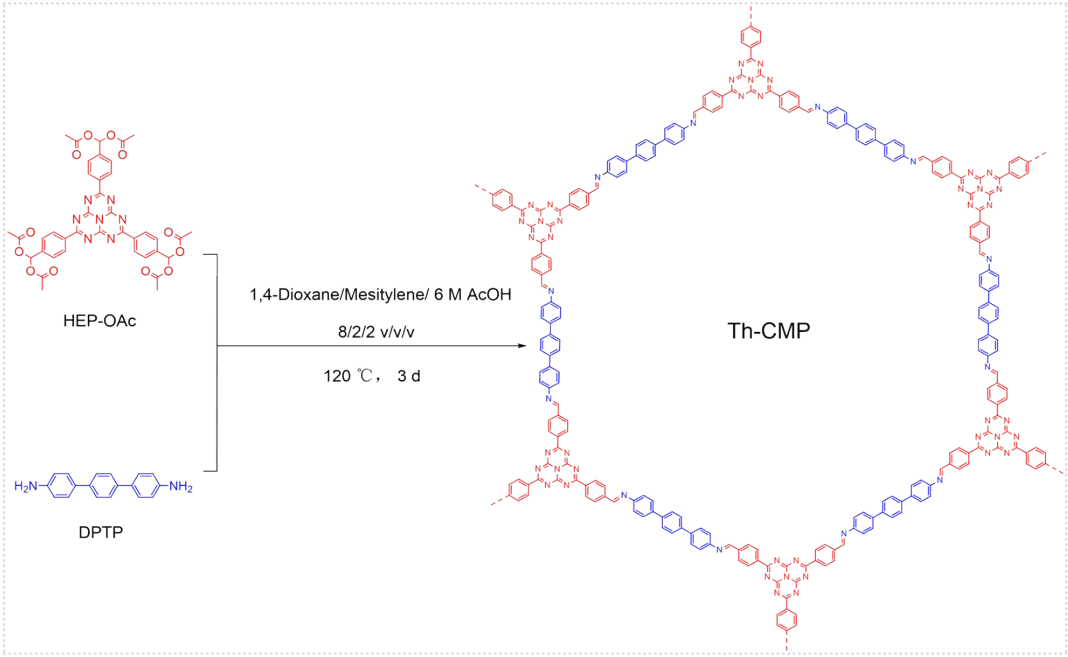

Scheme S3. Synthetic route of Th-CMP

3. Photocatalytic O_2 reduction experiments

The photocatalytic O_2 reduction reaction was carried out in a 16.5 mL glass photocatalytic reactor. Initially, 1 mg of the photocatalyst (Th-CMP or Tt-CMP) was accurately weighed and dispersed in 5 mL of deionized water in the reactor. The mixture was then ultrasonicated for 5 min to form a homogeneously dispersed suspension. Prior to irradiation, the reaction system was purged with high-purity O_2 (purity ≥ 99.99%) for 30 min to completely remove dissolved interfering gases (e.g., N_2, CO_2) and saturate the solution with O_2. Subsequently, the suspension was irradiated using a 300 W

xenon lamp equipped with a 400 nm cutoff filter (to ensure visible-light-only irradiation), and the incident light intensity was controlled at 100 mW cm^{-2} (measured by a light power meter). Throughout the experiment, the reactor was immersed in an ice-water bath to maintain a stable reaction temperature (ca. 0−5 °C) and minimize thermal effects. After the reaction, the generated products (primarily H_2O_2) were quantitatively analyzed by spectrophotometry based on the colorimetric method.

4. Photoelectrochemical measurements

All photoelectrochemical characterizations were conducted on a CHI760E electrochemical workstation using a standard three-electrode configuration. The working electrode was fabricated by modifying fluorine-doped tin oxide (FTO) conductive glass with the CMP samples, with an effective working area of 0.5 cm^2. The detailed fabrication process was as follows: 5 mg of the CMP sample was dispersed in 1 mL of ethanol to form a homogeneous ink via ultrasonication; 50 μL of the ink was then drop-cast onto the FTO surface and dried at 60 °C for 2 h under vacuum. An Ag/AgCl electrode (saturated with 3 M KCl solution) served as the reference electrode, and a platinum (Pt) sheet (1 cm × 1 cm) was used as the counter electrode. The electrolyte was 0.1 M Na_2SO_4 aqueous solution, which was purged with high-purity O_2 for 30 min prior to testing to achieve O_2 saturation. Under simulated visible-light irradiation, the photo response behavior and long-term stability of the CMP-based working electrodes were systematically evaluated by recording the photocurrent density-time (*I*−*t*) curves at a constant bias potential of −0.4 V *vs*. Ag/AgCl. Additionally, electrochemical impedance spectroscopy (EIS) measurements were carried out in the dark with an AC voltage amplitude of 5 mV and a frequency range of 1 Hz to 10^5 Hz. These EIS measurements were used to investigate the interfacial charge transfer and separation properties of the CMP electrodes.

5. Product analysis

The quantification of the photocatalytic O_2 reduction product (H_2O_2) was performed using the potassium iodide (KI) colorimetric method. A calibration curve (linear relationship between H_2O_2 concentration and absorbance) was first constructed as follows: gradient concentrations of H_2O_2 standard solutions (0−490 μM) were prepared; 1 mL of each standard solution was mixed with 0.5 mL of 0.2 M potassium hydrogen phthalate (KHP) buffer solution (pH = 4.0, to maintain a stable acidic environment for color development) and 0.5 mL of 0.1 M KI solution. After standing in the dark for 30 min (to ensure complete color development), the absorbance of each mixture was measured at 350

nm using a UV−Vis spectrophotometer. For the analysis of reaction samples, 1 mL of the filtered reaction solution (through a 0.22 μm PTFE membrane to remove the photocatalyst) was collected and treated with the same reagents and procedures as the standard solutions. The H_2O_2 concentration in the sample was calculated using the linear fitting equation of the calibration curve, and the photocatalytic activity of the two CMP materials was evaluated based on the H_2O_2 yield.

6. Water contact angle measurements

Water contact angle measurements were performed on a SZ-CAMC33 contact angle analyzer. Prior to measurement, all samples were compacted into uniform tablets to ensure a smooth and flat surface, which is critical for reliable contact angle data. The as-prepared samples were placed on the test stage. All tests were conducted at room temperature (25 ± 1 °C) and ambient humidity (50 ± 5% RH). The testing liquid was deionized water with a resistivity of 18.2 MΩ·cm, and the droplet volume was fixed at 0.2 μL. Static water contact angles were determined using the sessile drop method, and the ring method was also applied to further confirm and validate the measured contact angles, ensuring the accuracy and reproducibility of the results. These standardized parameters are clearly presented in the *Water contact angle measurements* section of the supplementary materials.

7. Operando FTIR spectroscopy measurements

Operando Fourier transform infrared (FTIR) spectroscopy measurements were carried out at room temperature using a Nicolet iS50 FT-IR spectrometer (Thermo Scientific) equipped with a liquid nitrogen-cooled mercury cadmium telluride (MCT) detector, coupled with an in-situ reaction cell (Model CRCP-7070-CLT, Tianjin Xianquan Industry and Trade Co., Ltd.). Prior to testing, 1 mg of the CMP sample was thoroughly ground and mixed with 200 mg of spectroscopically pure KBr, and the mixture was pressed into a thin pellet for FTIR measurement. The system was first degassed under vacuum to remove residual air, followed by purging with a stream of O_2 (purity ≥ 99.99%) and H_2O vapor for 20 min to establish the reaction atmosphere. After allowing the system to stabilize under the above atmosphere for 30 min, the background spectrum was collected under the same gas flow and temperature conditions. Finally, the light source was turned on, and the operando FTIR spectra of the sample were recorded with a wavenumber range of 4000−400 cm^{-1}.

8. AQY measurement of H_2O_2 Production

To determine the apparent quantum yield (AQY), photocatalytic reactions were conducted using

a multi-channel light panel equipped with multiple single-wavelength LEDs. The LED wavelengths were set to 425, 450, 470, and 530 nm, with a fixed illumination area of 0.28 cm^2 and an irradiation time of 30 minutes. To ensure accurate AQY calculation, the light intensity at each wavelength was measured using an optical power meter. The AQY was calculated according to the standard formula.

$$AQY = \frac{N_e}{N_p} = \frac{2 \times N \times N_A \times h \times c}{S \times I \times t \times \lambda} \times 100\%$$

In the equation, N is the yield of H_2O_2 (mol), N_A is Avogadro's constant (6.02×10^{23} mol^{-1}), h is Planck's constant (6.626×10^{-34} $J \cdot s^{-1}$), c is the speed of light (3×10^8 $m \cdot s^{-1}$), S is the irradiation area (0.28 cm^2), I is the light intensity ($W \cdot cm^{-2}$), t is the photoreaction time (1800 s), and λ is the wavelength of the monochromatic light (nm).

9. Solar-to-chemical conversion (SCC) efficiency

The solar-to-chemical conversion (SCC) efficiency was determined by irradiating 5 mg of the catalyst for 30 min using a 300 W xenon lamp with a light intensity of 80 mW cm^{-2}.

$$SCC = \frac{\Delta G_{H_2O_2} \times n}{S \times I \times t} \times 100\%$$

In the equation, $\Delta^{G_{H_2O_2}}$is the free energy for H_2O_2 generation (117 kJ mol^{-1}), n is the amount of H_2O_2 produced (mol), S is the irradiation area (1.5 cm^2), I is the light intensity (80 mW cm^{-2}), and t is the irradiation time (1800 s).

10. DFT calculation

The electrostatic potential (ESP) of triazine- and heptazine-based fragments was calculated to evaluate their electron-deficient characters using Materials Studio 2023 software (MS). First, molecular models of the triazine and heptazine core fragments were constructed separately. Subsequently, the electrostatic potential of the two fragments was calculated using the DMol3 module embedded in MS. The calculation parameters were set as follows: the task was geometry optimization, the functional was GGA-PBE, the basis set was DNP, the charge was 0 (electrically neutral). The electron density and electrostatics were selected in the properties to obtain the ESP data. After the calculation was completed, the ESP maps were visualized and analyzed to compare the electron distribution differences between the two fragments.

11. Characterization

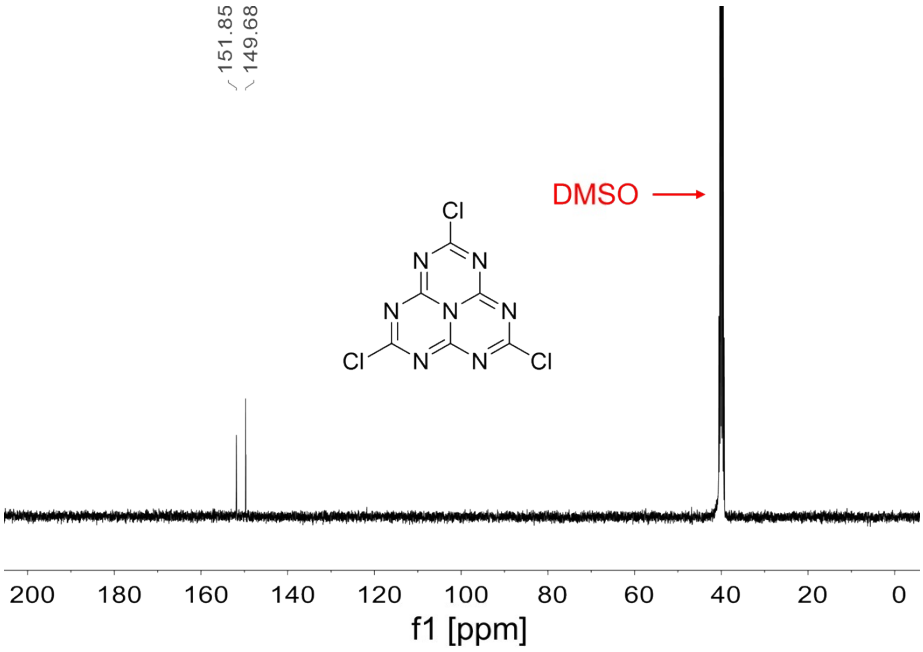

Fig. S1 ^{13}C NMR spectrum of cyameluric chloride (100 MHz, DMSO-d_6).

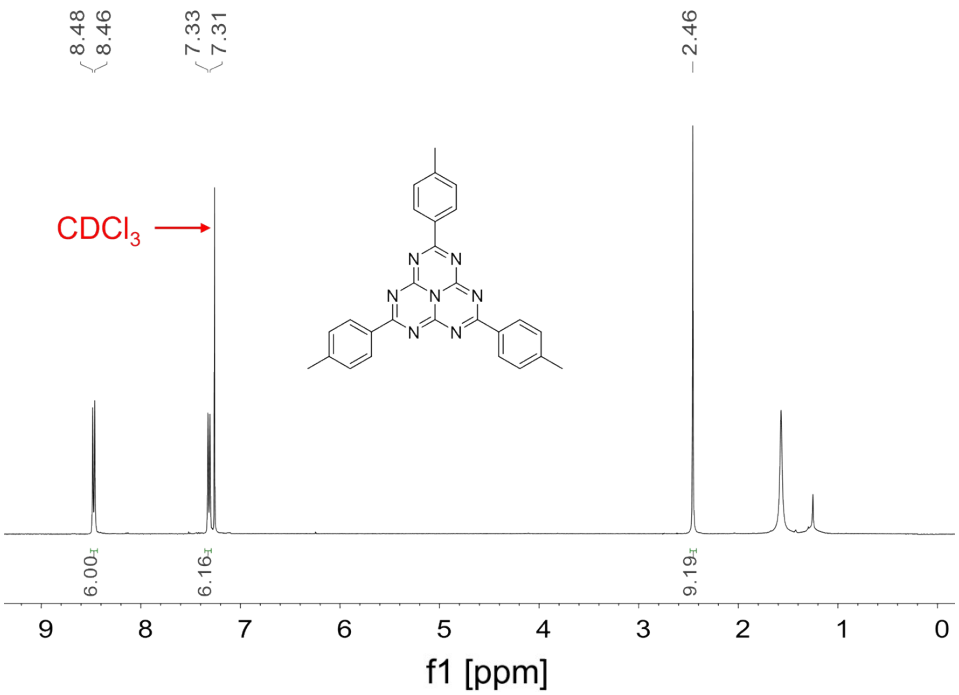

Fig. S2 ^{1}H NMR spectrum of tris-(4-tolyl)- tri-s-triazine (400 MHz, $CDCl_3$).

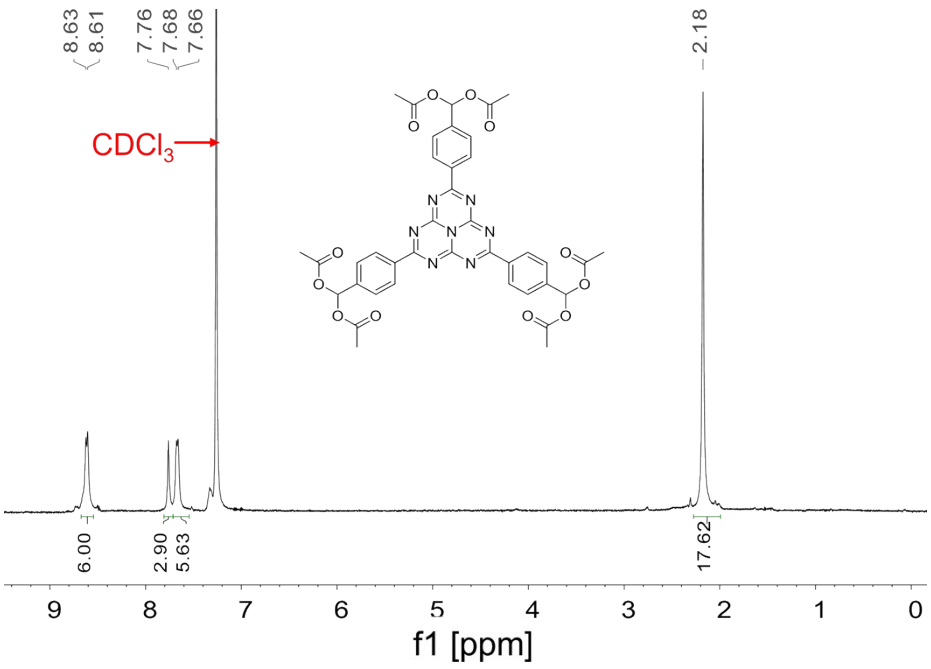

Fig. S3 ^{1}H NMR spectrum of HEP-OAc (400 MHz, $CDCl_3$).

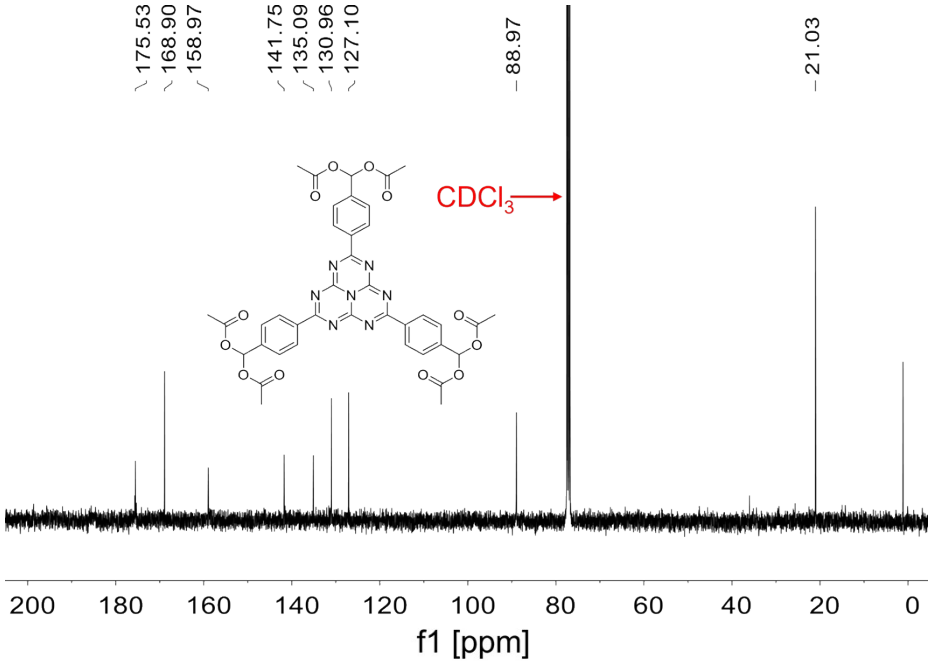

Fig. S4 ^{13}C NMR spectrum of HEP-OAc (100 MHz, $CDCl_3$).

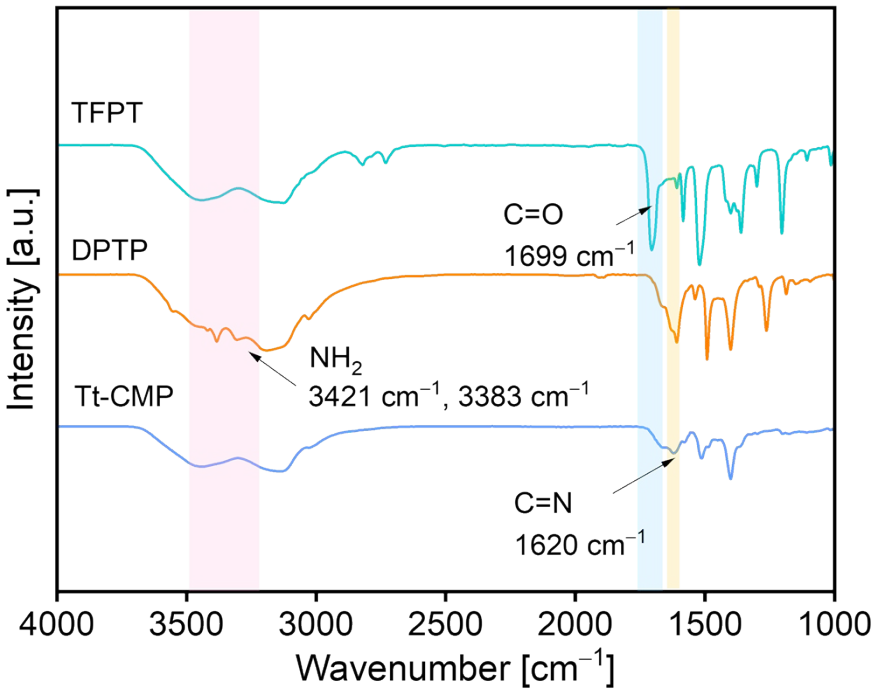

Fig. S5 FT-IR spectra of Tt- CMP (blue), TFPT, and DPTP (orange).

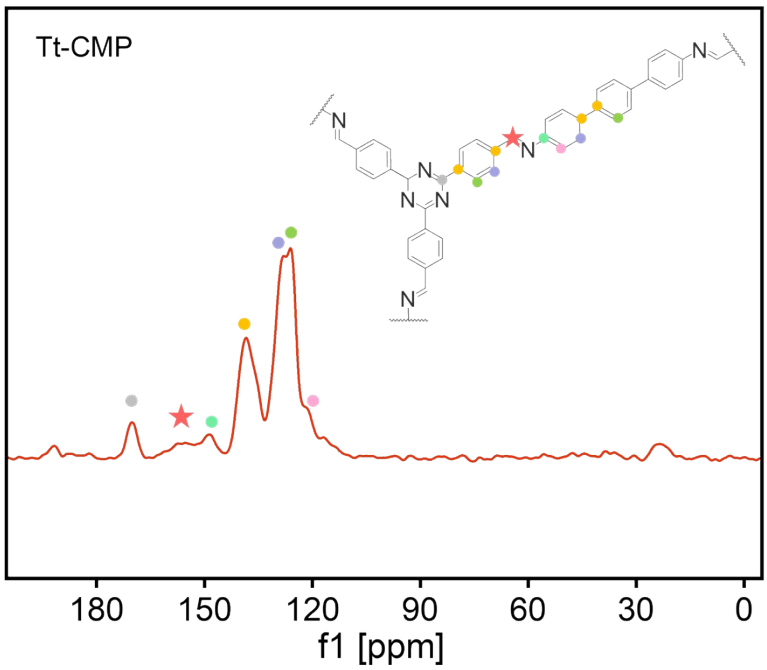

Fig. S6 ^{13}C solid-state NMR spectrum of Tt- CMP.

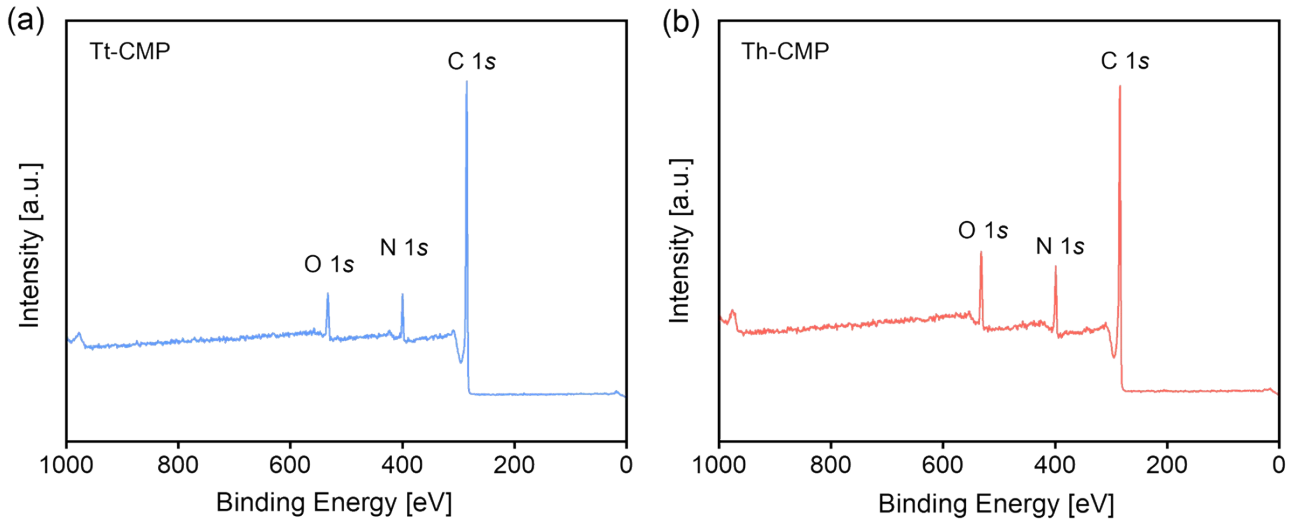

Fig. S7 Survey scan XPS profiles of Tt-CMP and Th-CMP.

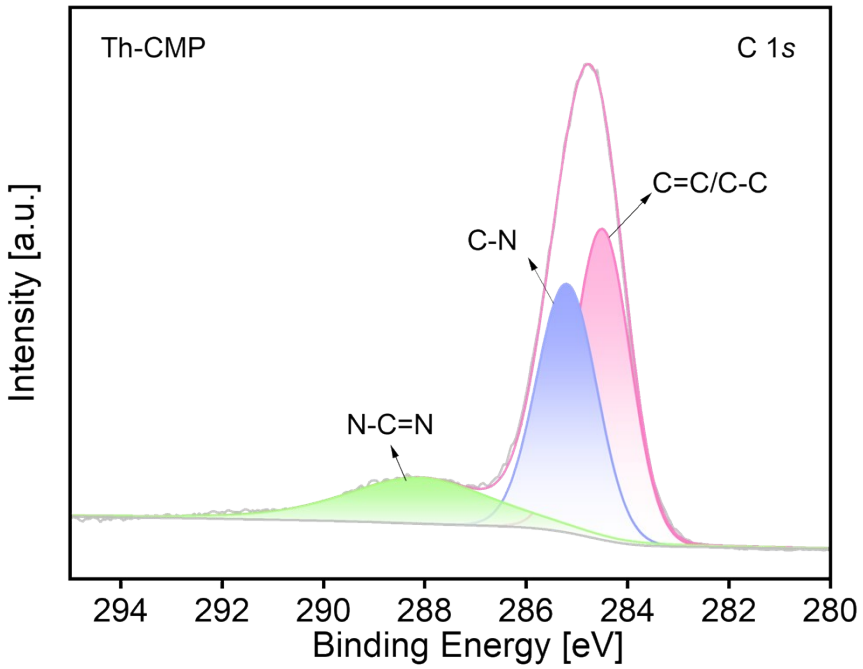

Fig. S8 High-resolution C 1*s* XPS spectrum of Th-CMP.

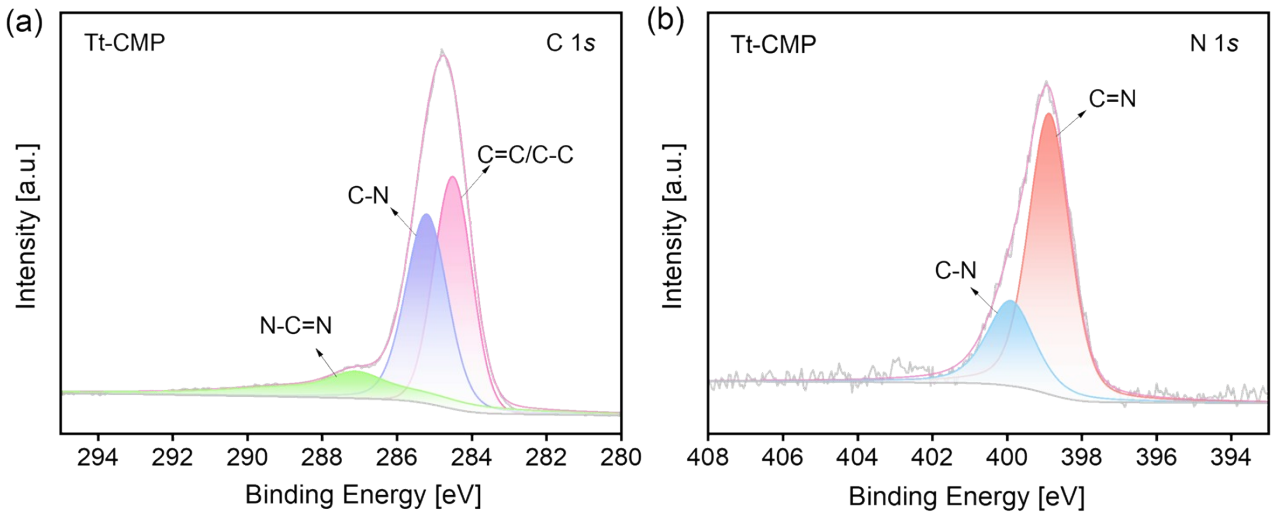

Fig. S9 High-resolution XPS spectra of Tt-CMP: (a) C 1*s* and (b) N1*s*.

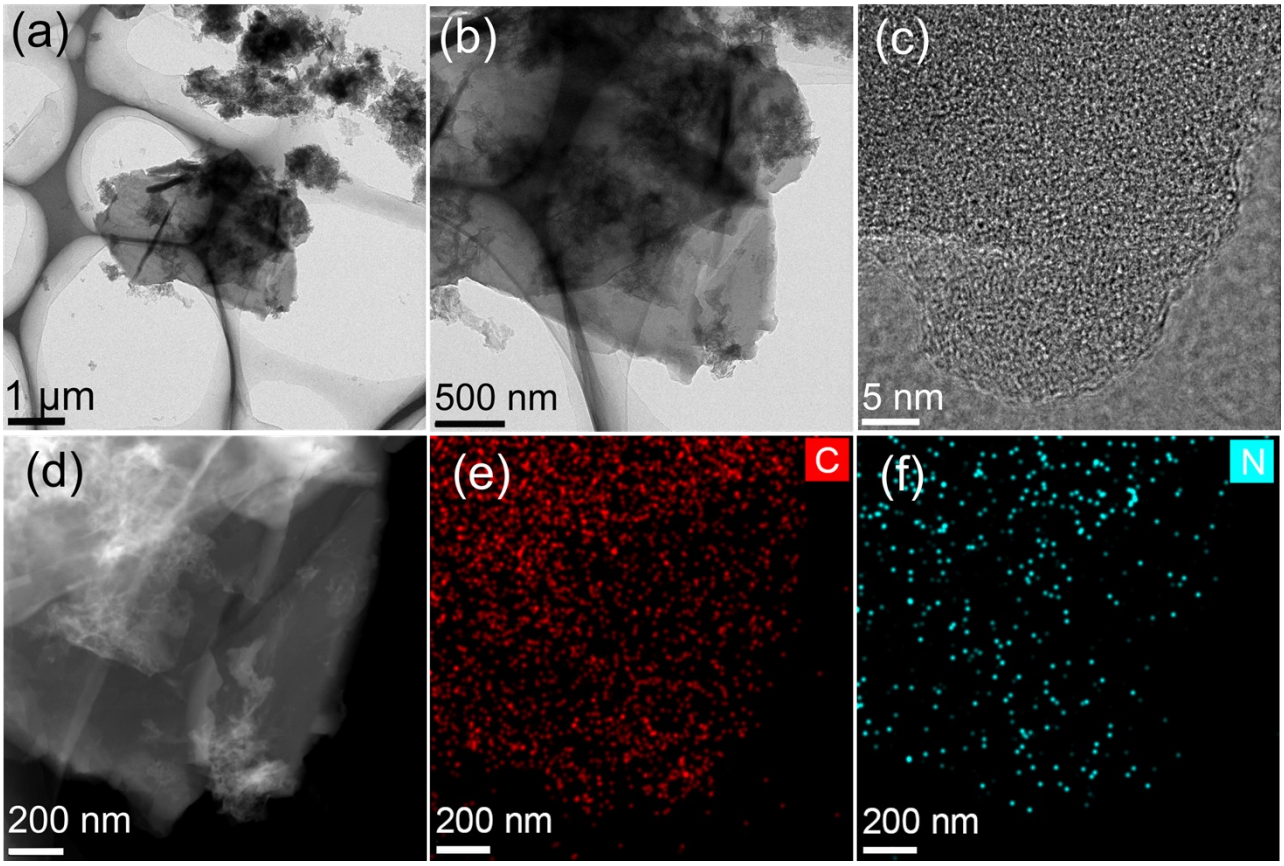

Fig. S10 HRTEM and EDS mapping images of Th-CMP.

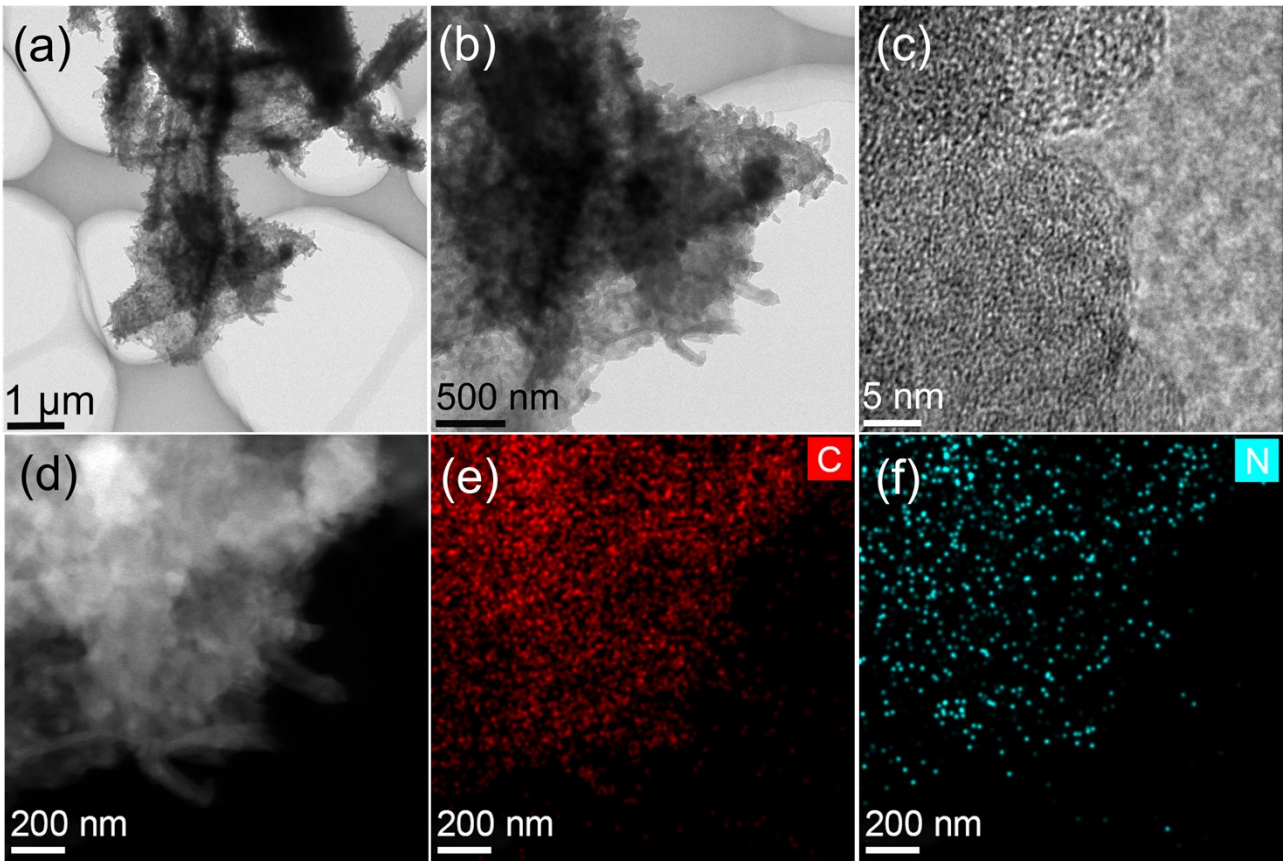

Fig. S11 HRTEM and EDS mapping images of Tt-CMP.

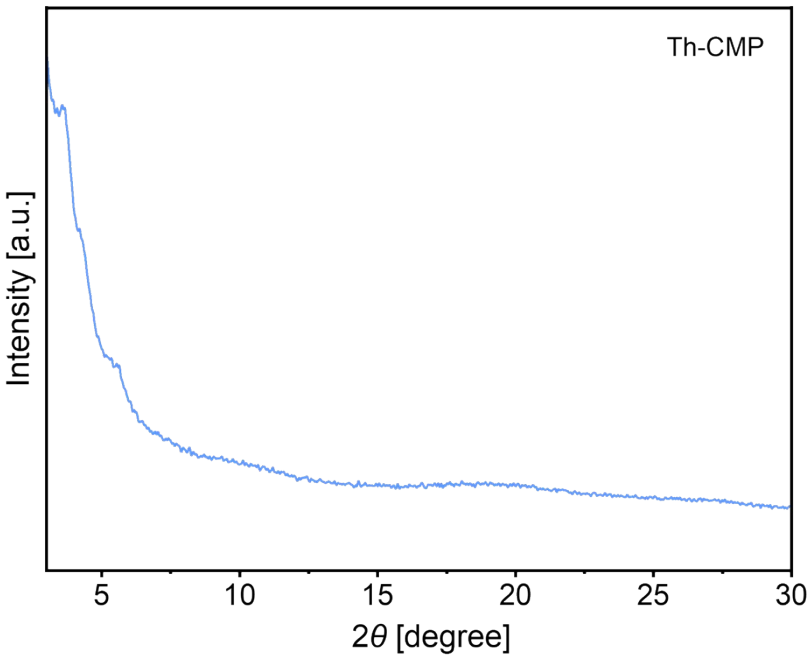

Fig. S12 Powder X-ray diffraction pattern of Tt-CMP

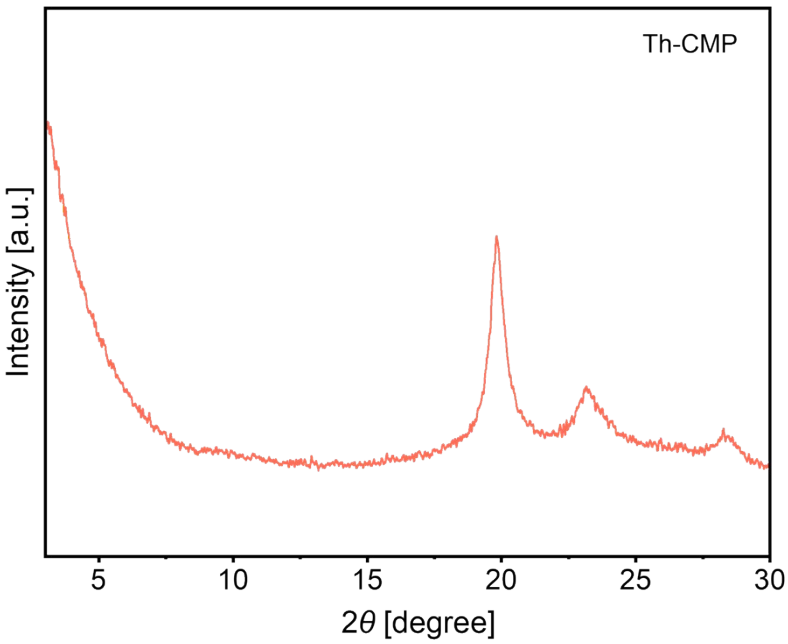

Fig. S13 Powder X-ray diffraction pattern of Th-CMP.

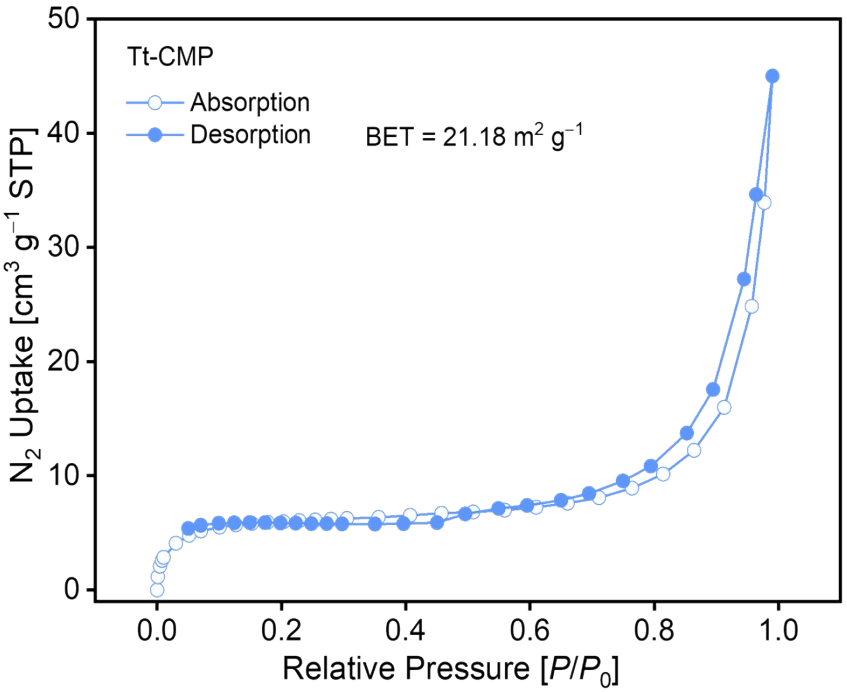

Fig. S14 N_2 adsorption−desorption isotherms and surface area of Tt-CMP at 77 K.

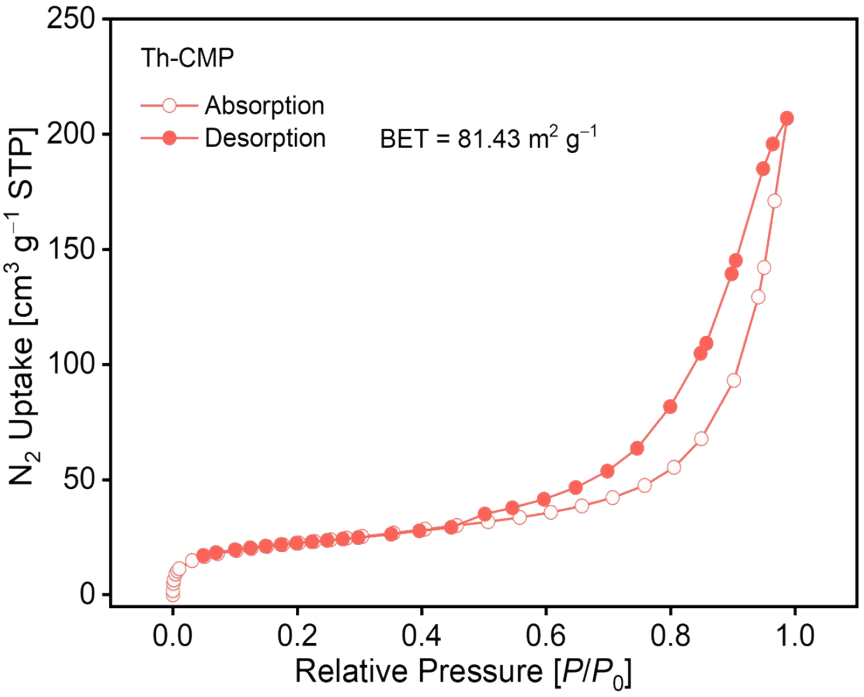

Fig. S15 N_2 adsorption−desorption isotherms and surface area of Th-CMP at 77 K.

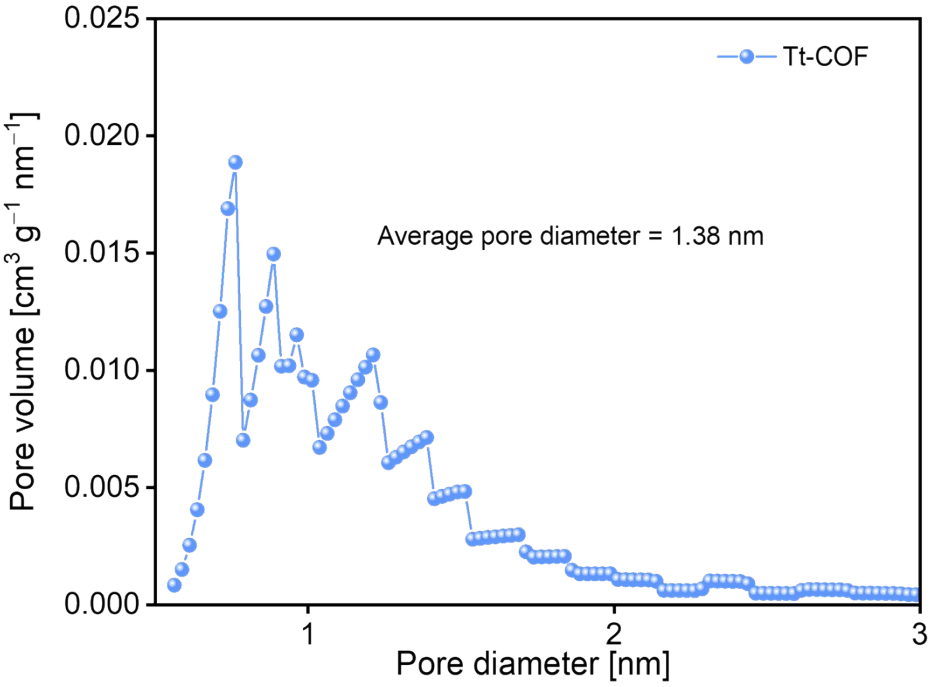

Fig. S16 Average pore diameter of Tt-CMP.

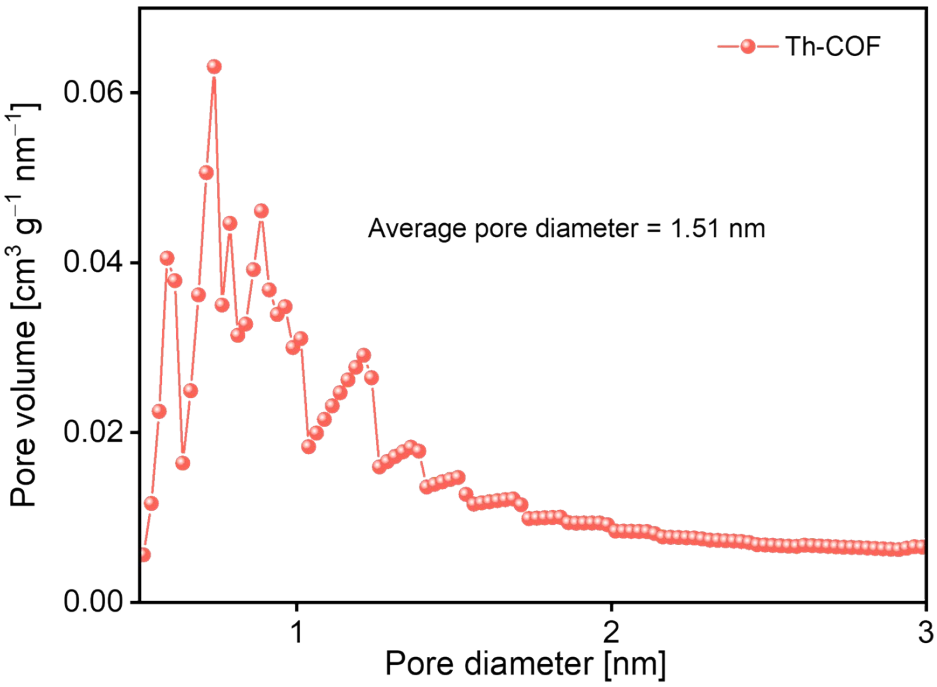

Fig. S17 Average pore diameter of Th-CMP.

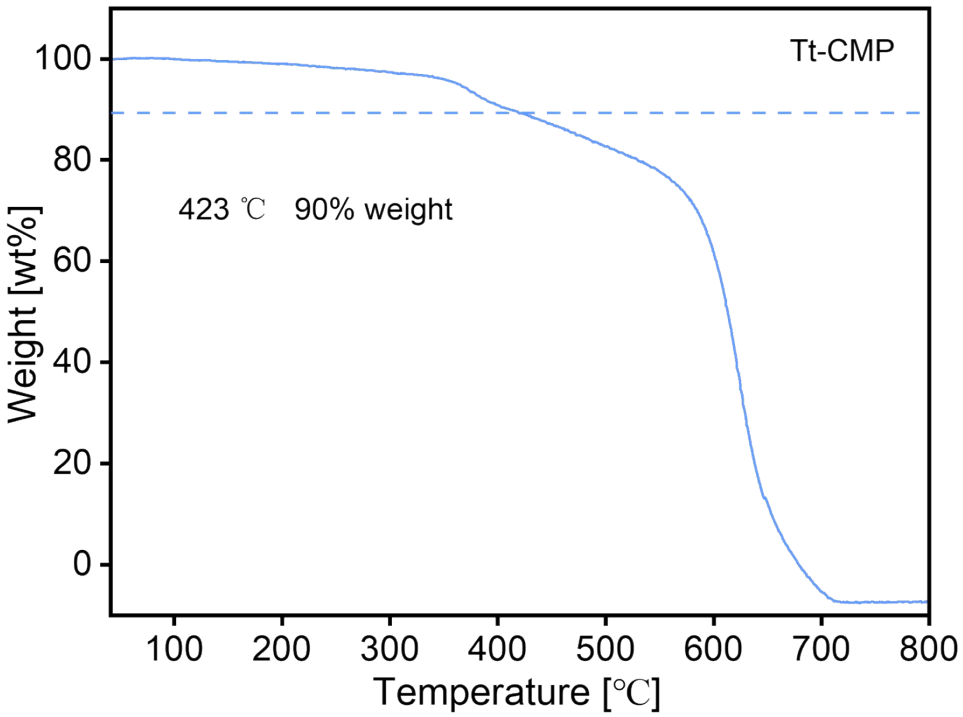

Fig. S18 TGA curve of Tt-CMP under Ar atmosphere.

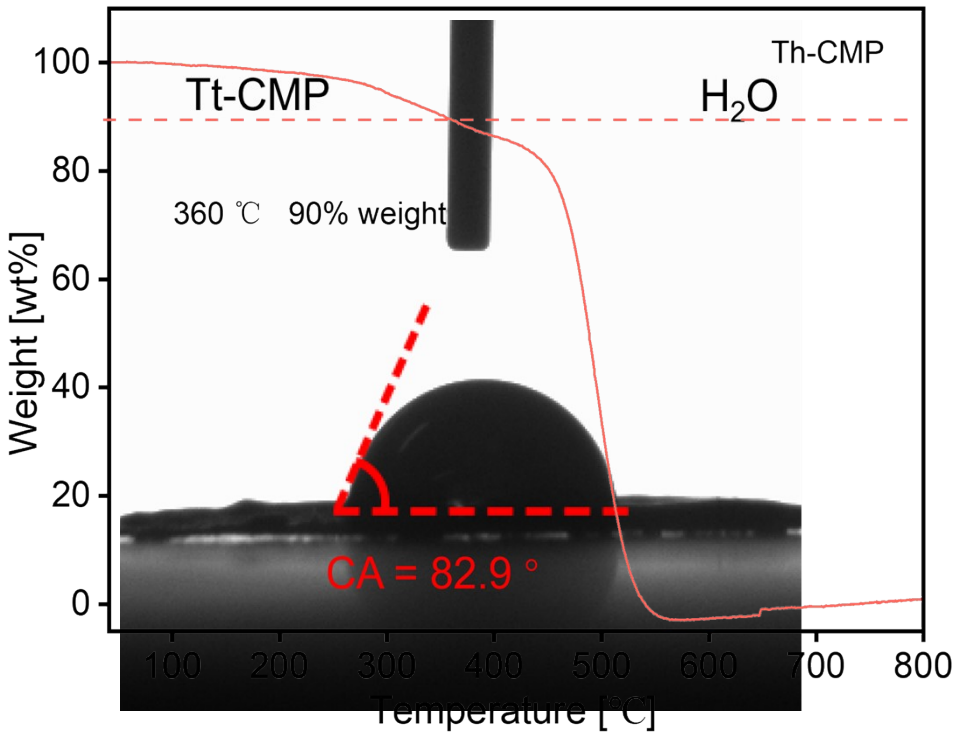

Fig. S19 TGA curve of Th-CMP under Ar atmosphere.

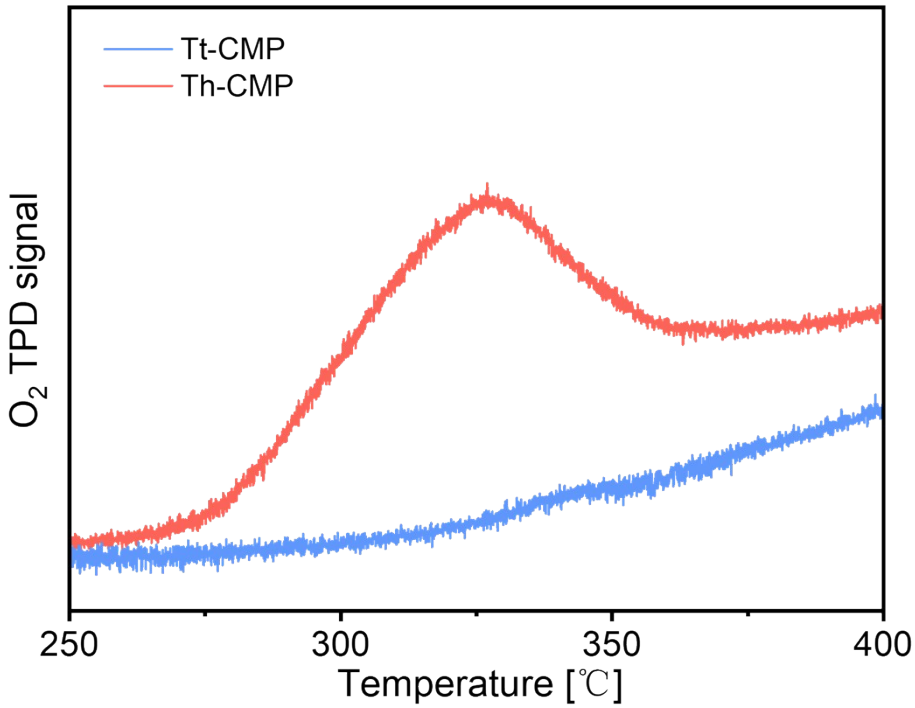

Fig. S22 O_2 TPD plots of Th-CMP and Tt-CMP.

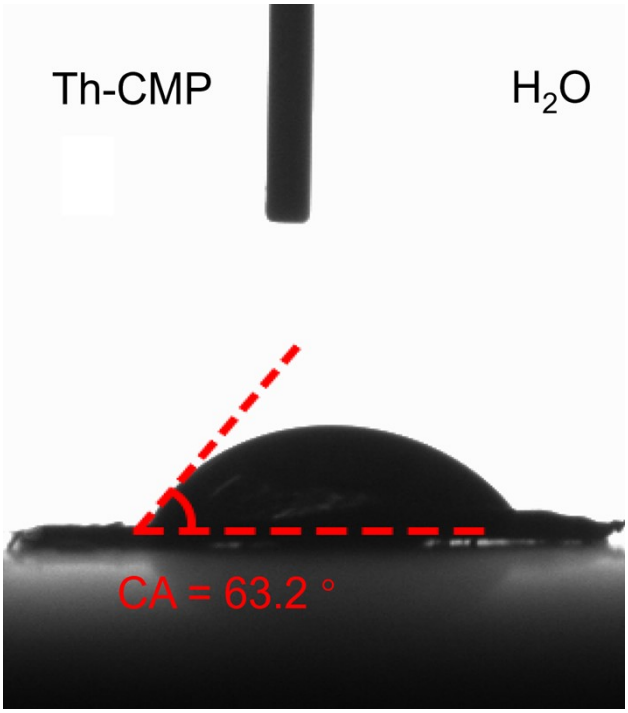

Fig. S21 The water contact angle of Th-CMP.

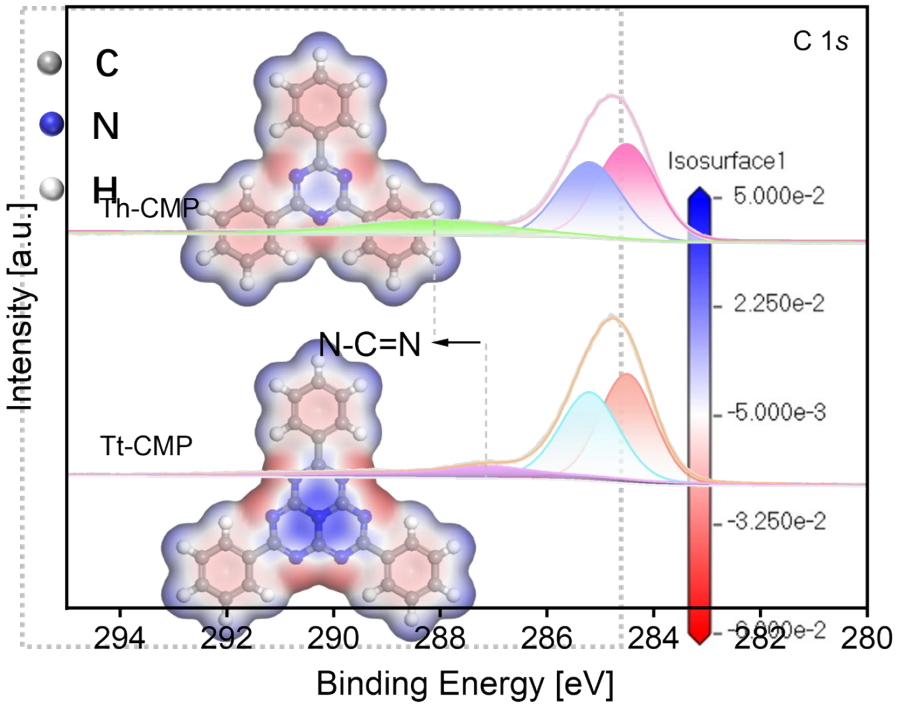

Fig. S23 The C 1*s* high-resolution XPS spectra of Tt-CMP and Th-CMP.

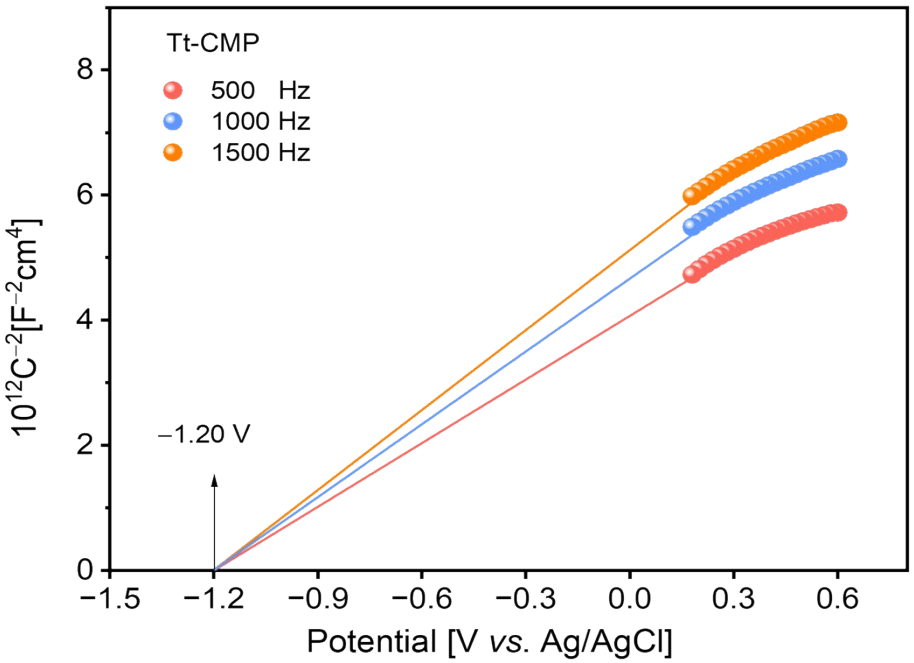

Fig. S25 Mott−Schottky plots of Tt-CMP.

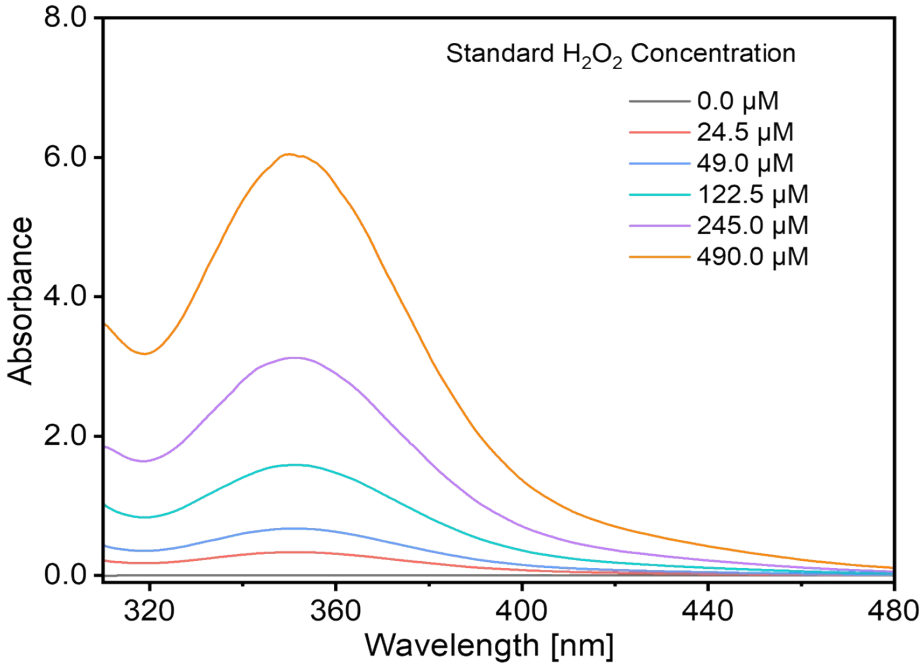

Fig. S26 UV−Vis absorption spectra of standard H_2O_2 solutions at different concentrations.

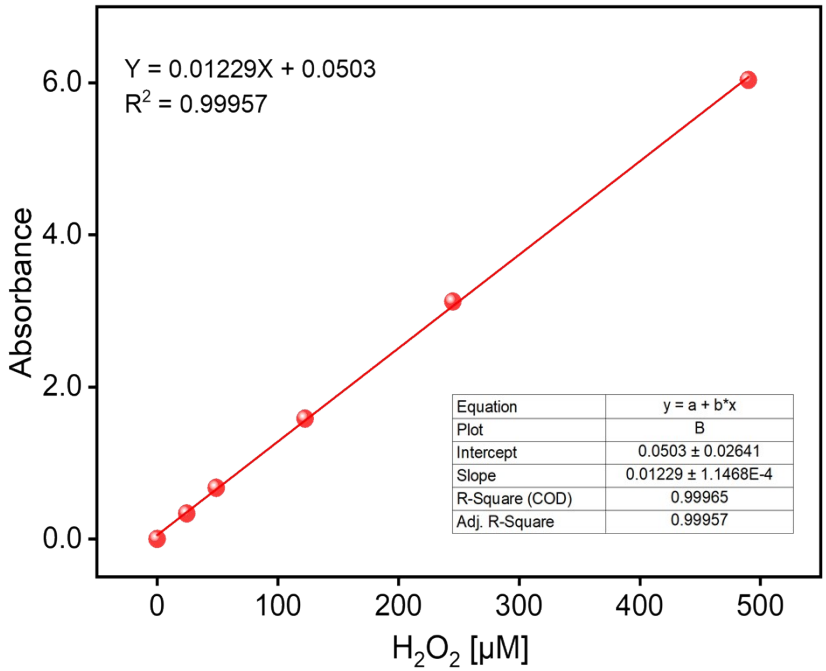

Fig. S27 Linear calibration curve for H_2O_2 quantification: experimental data and fitted line with equation.

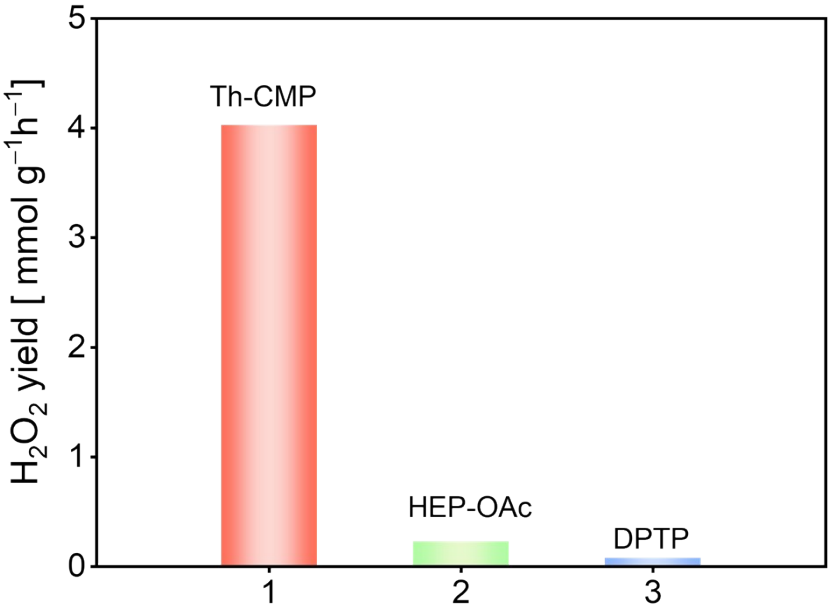

Fig. S28 H_2O_2 generation yields of Th-CMP, HEP-OAc and DPTP.

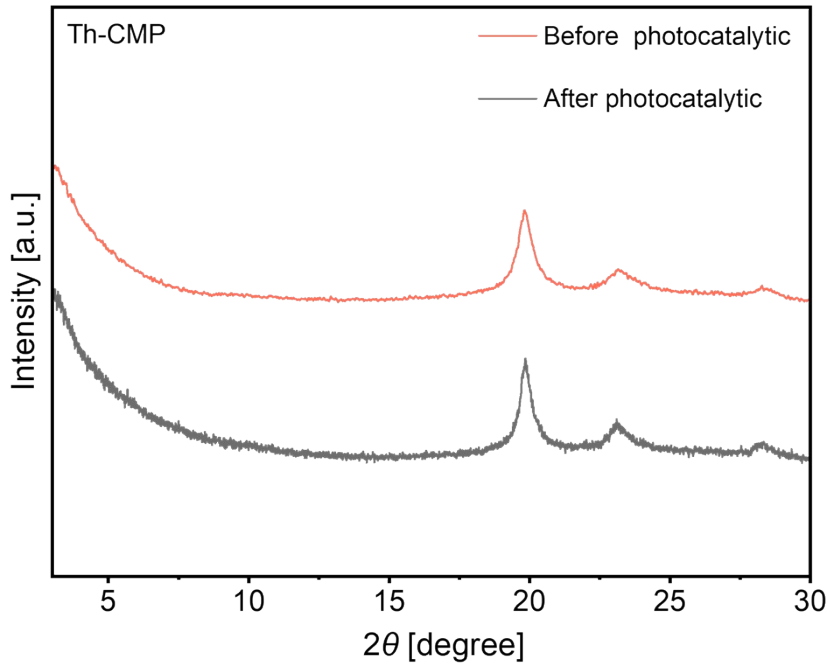

Fig. S29 PXRD patterns of Th-CMP before and after recycling experiments.

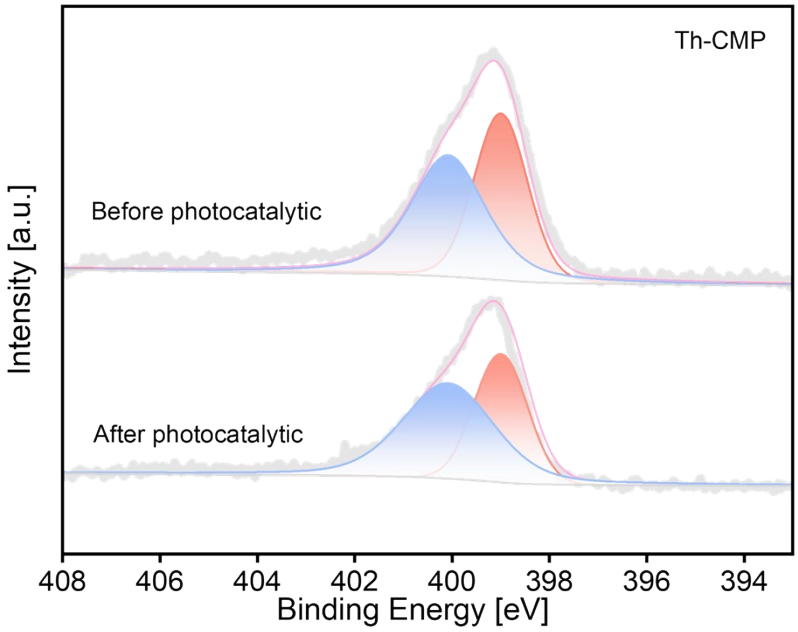

Fig. S30 XPS patterns of Th-CMP before and after recycling experiments.

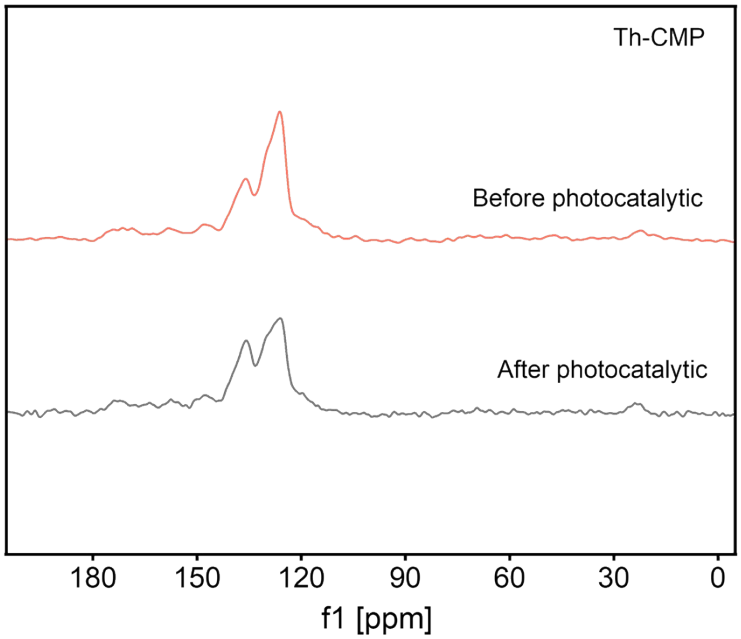

Fig. S31 NMR patterns of Th-CMP before and after recycling experiments.

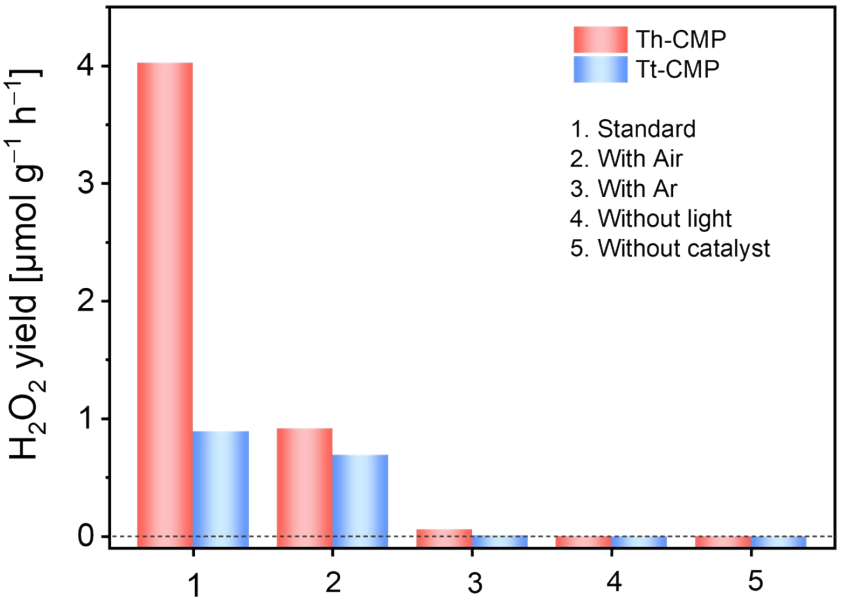

Fig. S32 H_2O_2 generation yields of Tt-CMP and Th-CMP under different reaction conditions.

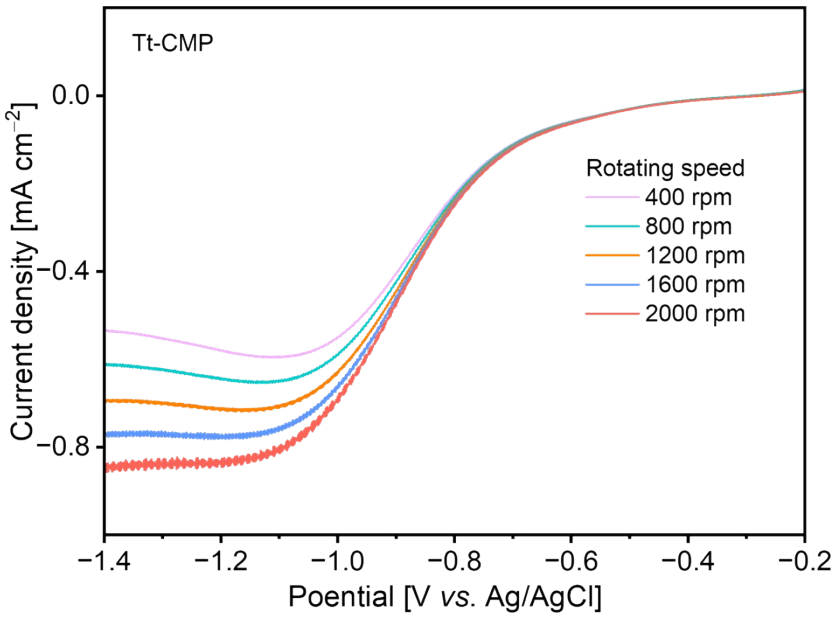

Fig. S33 Linear sweep voltammetry (LSV) curve for the oxygen reduction reaction (ORR) on a Tt-CMP modified rotating disk electrode (RDE).

12. References

1 D. Chen, W. B. Chen, G. Zhang, S. Li, W. Chen, G. Xing and L. Chen, *ACS Catal*., 2021, **12**, 996−1004.

2 L. Maxwell, S. Gómez-Coca, T. Weyhermüller, D. Panyella and E. Ruiz, *Dalton Trans*., 2015, **44**, 15761−15763.

3 P. Kumar, E. Vahidzadeh, U. K. Thakur, P. Kar, K. M. Alam, A. Goswami, N. Mahdi, K. Cui, G. M. Bernard, V. K. Michaelis and K. Shankar, *J. Am. Chem. Soc*., 2019, **141**, 5415−5436.

4 Y. Ke, D. J. Collins, D. Sun and H.-C. Zhou, *Inorg. Chem*., 2006, **45**, 1897−1899.